Pictorial Essay

Gadolinium-Enhanced MR Angiography: Artifacts and Pitfalls

Vivian S. Lee [1], Doug J. Martin, Glenn A. Krinsky, Neil M. Rofsky

G adolinium-enhanced MR angiography for evaluation of vessels is relatively noninvasive and safe. A growing body of literature supports its accuracy compared with that of conventional contrast angiography [1]. Our purpose is to review the imaging pitfalls and artifacts of this method that may be encountered in the clinical setting. Knowledge of these potential problems is essential for accurate image interpretation; an awareness of their causes can suggest better imaging strategies.

Gadolinium-Enhanced MR Angiography Technique

MR imaging was performed on a 1.5-T system (Vision or Symphony; Siemens, Erlangen, Germany). Three-dimensional spoiled gradient-echo images were acquired with a torso phased array coil for chest and abdominal applications and with a coil for peripheral vascular imaging, with the following parameters (TR range/TE range, 3.8–5/1.3–2; flip angle, 25–40°). Peripheral MR angiography was performed with either single- or multistation bolus-chase methods. Typical fields of view ranged from 300 to 450 mm with an in-plane matrix of 256–512 $\times$ 128–160 with a rectangular field of view depending on patient body habitus. Sinc interpolation was used to provide isotropic pixel size of less than 2.5 mm. Acquisition times were kept less than 25 sec to facilitate breath-holding, which was performed at end-expiration for best reproducibility.

The three-dimensional acquisitions were performed both before and after the administration of 0.1–0.2 mmol/kg gadolinium contrast material (Magnevist; Berlex Laboratories, Wayne, NJ) with the contrast-enhanced study timed with a
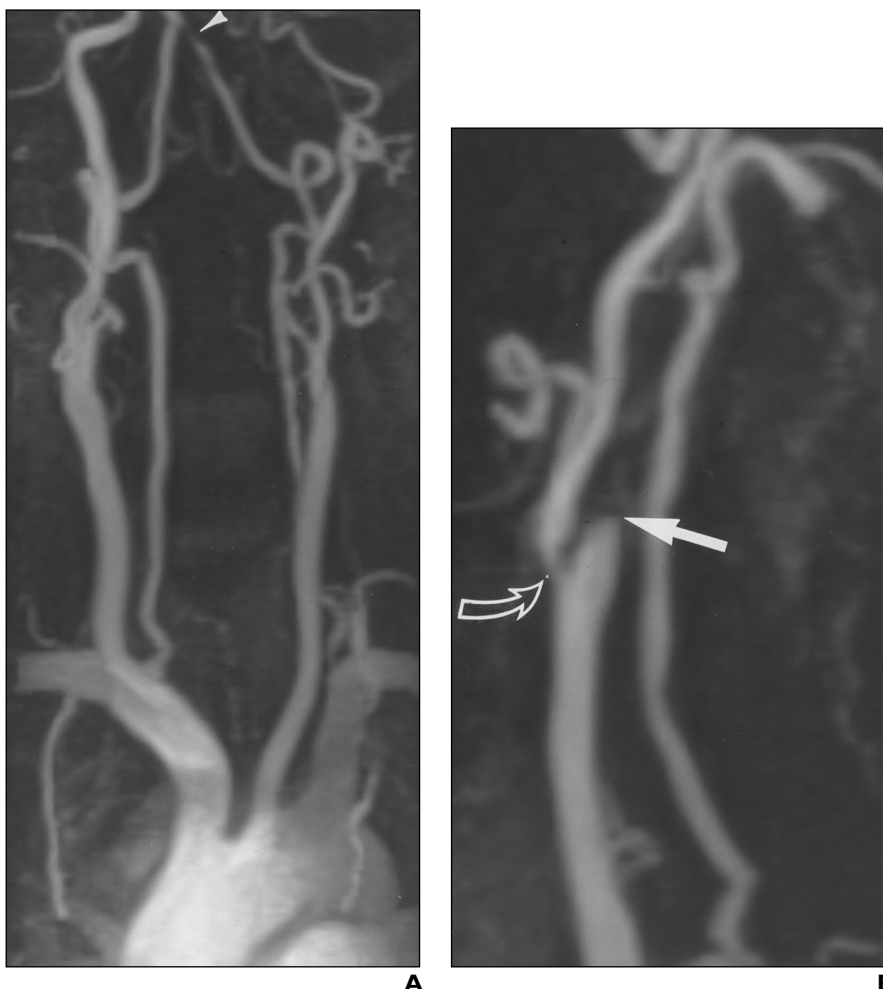

A
B

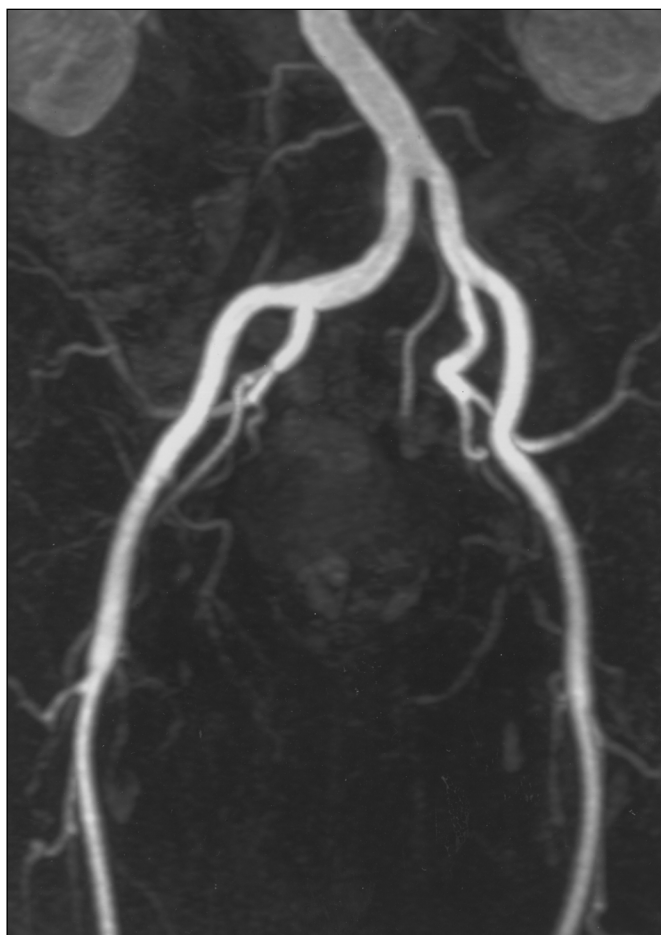**Fig. 1.**—69-year-old man with left internal carotid artery stenosis.
A, Coronal maximum intensity projection of gadolinium-enhanced MR angiogram shows substantial arterial enhancement with virtually no venous enhancement. Note mild narrowing of distal left vertebral artery (*arrowhead*). Timing of acquisition was set to coincide with arterial enhancement on basis of test-bolus timing examination.
B, Oblique sagittal subvolume maximum intensity projection of MR angiogram reveals focal high-grade stenosis of left internal carotid artery (*solid arrow*). Source images (not shown) confirmed faint signal within left internal carotid artery beyond stenosis. Note mild narrowing at origin of left external carotid artery (*open arrow*).
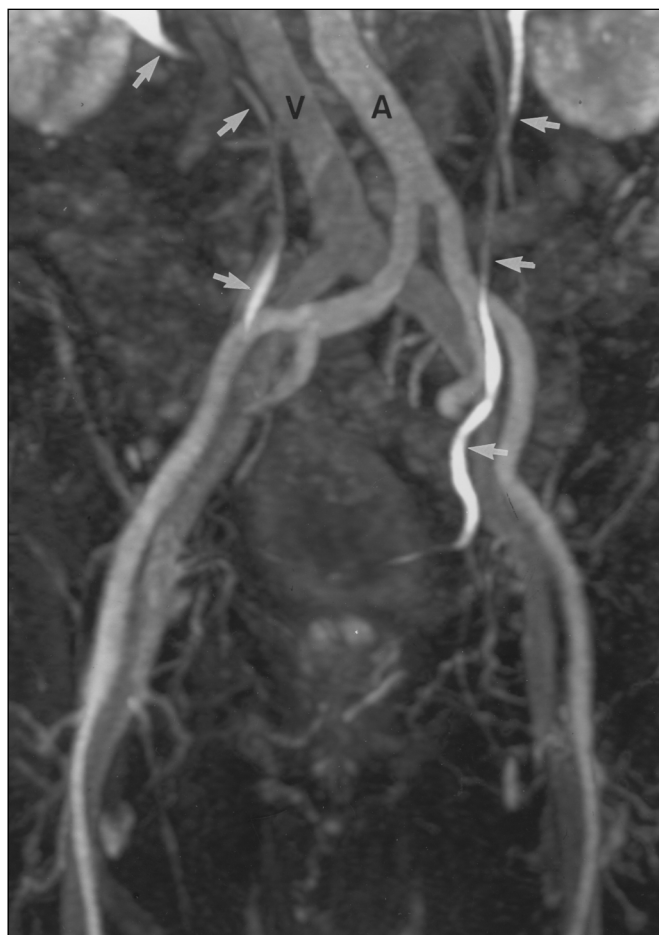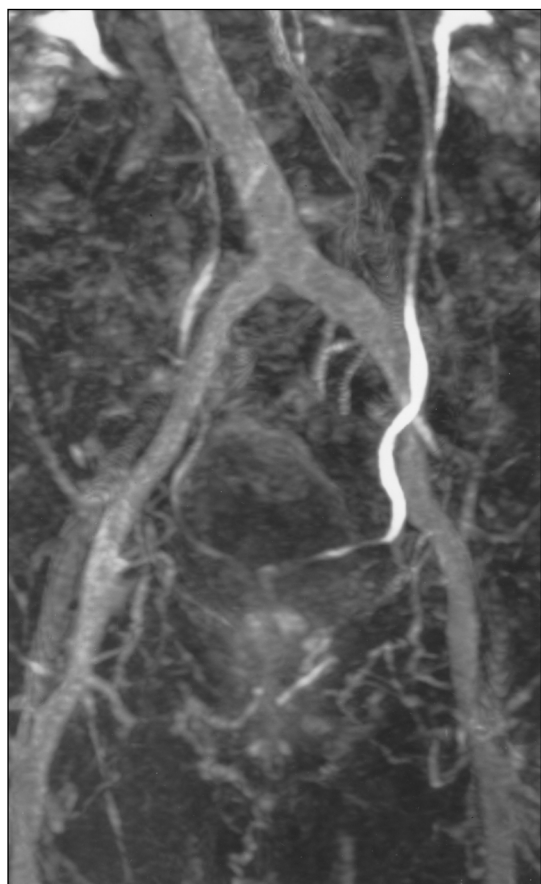
Fig. 2.—Venous enhancement in 69-year-old man with suspected venous occlusion.

A, Coronal maximum intensity projection of gadolinium-enhanced MR angiogram, timed using test bolus of contrast material, reveals normal arterial anatomy in pelvis.

**B**, Coronal maximum intensity projection of similar acquisition obtained 20 sec after **A** shows enhancement of both aorta (A) and inferior vena cava (V) and is representative of acquisition obtained after peak arterial enhancement and during recirculation. Note concentrated contrast material in ureters (*arrows*) caused by timing examination with earlier test bolus.

C, Coronal maximum intensity projection of data set obtained by subtracting **A** from **B** reveals normal MR venogram [5].

Fig. 3.—Unilateral early venous enhancement in 73-year-old man with left lower extremity claudication. Coronal maximum intensity projection of gadolinium-enhanced MR angiogram shows focal high-grade stenosis at left common femoral artery (*long solid arrow*) and both superficial femoral arteries (*short solid arrows*). Asymmetric early venous enhancement (*open arrows*) extending proximally from right superficial femoral artery suggests unsuspected arteriovenous fistula. Patient had recently undergone right femoral catheterization.
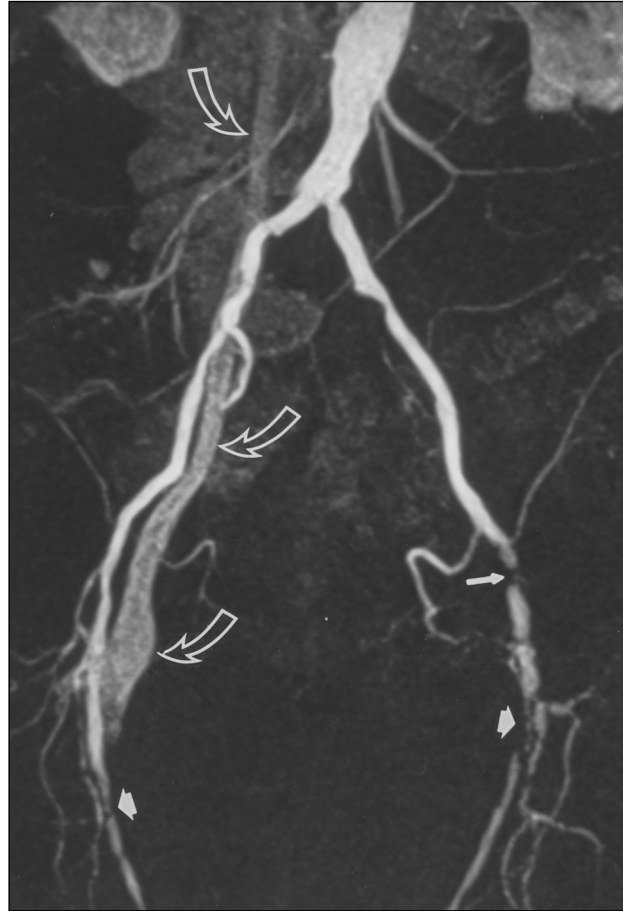
Fig. 4.—Artifact resulting from data acquisition before arrival of contrast bolus in aorta in 53-year-old woman with suspected mesenteric ischemia. Coronal source image from gadolinium-enhanced MR angiogram of abdominal aorta shows characteristic appearance of "Maki" artifact in which edges of vessel appear enhanced whereas central regions do not. This appearance results from bolus arriving in aorta after central (contrast-determining low spatial frequency) lines of K-space have been collected while peripheral (high spatial frequency) lines that determine edge contrast are collected after contrast enhancement [6].
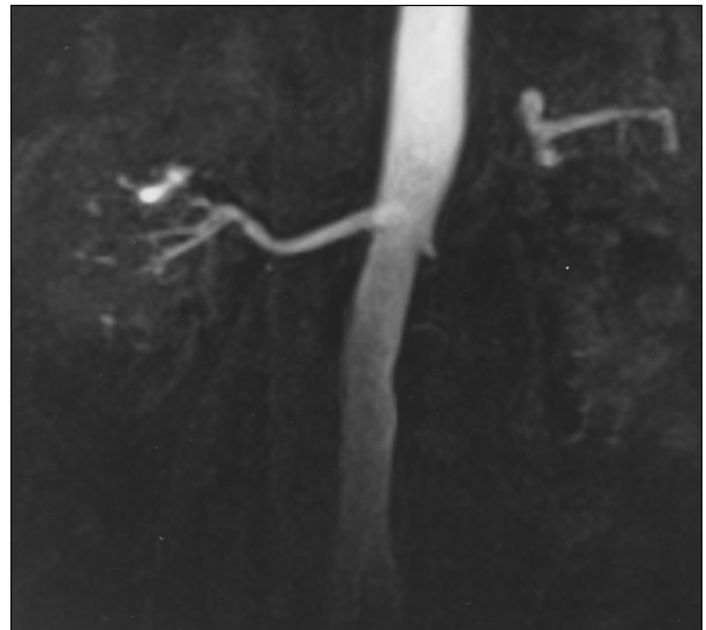

3
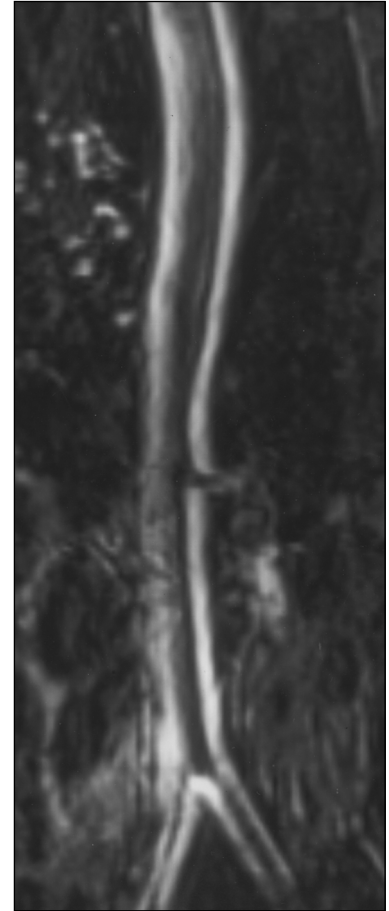
4

Fig. 5.—Mistimed MR angiogram causing mild artifact in 67-year-old man examined for follow-up after left nephrectomy for renal cell carcinoma. Coronal maximum-intensity-projection image shows contrast-enhanced edges of infrarenal aorta with central unenhanced regions that result from MR images being acquired before arrival of high concentration of contrast agent into aorta.
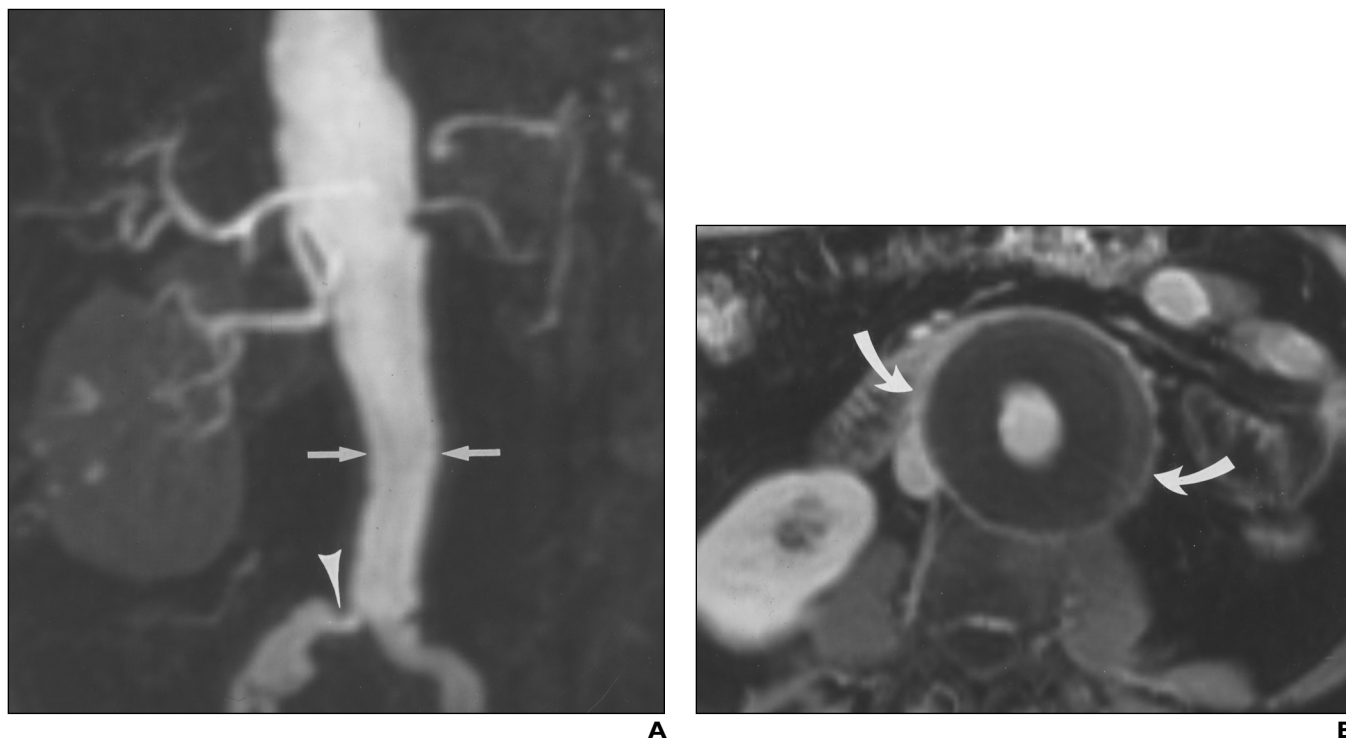
A

B

Fig. 6.—Infrarenal abdominal aortic aneurysm underestimated by maximum intensity projection of gadolinium-enhanced MR angiogram in 63-year-old woman with pulsatile abdominal mass.

A, Coronal maximum intensity projection of gadolinium-enhanced MR angiogram shows widened suprarenal and juxtarenal aorta with normal-caliber infrarenal aorta (*arrows*). Note right common iliac artery stenosis (*arrowhead*).

B, Fat-suppressed axial T1-weighted gradient-echo image (TR/TE, 160/2.3; flip angle, 80°) obtained through infrarenal aorta after contrast-enhanced MR angiography shows 7.2-cm aneurysm (*arrows*) with circumferential mural thrombus that is not well visualized on **A**. Like conventional angiography, MR angiography is luminal technique. To evaluate for extraluminal abnormality, it is important to perform T1-weighted imaging after all contrast-enhanced abdominal MR angiography.
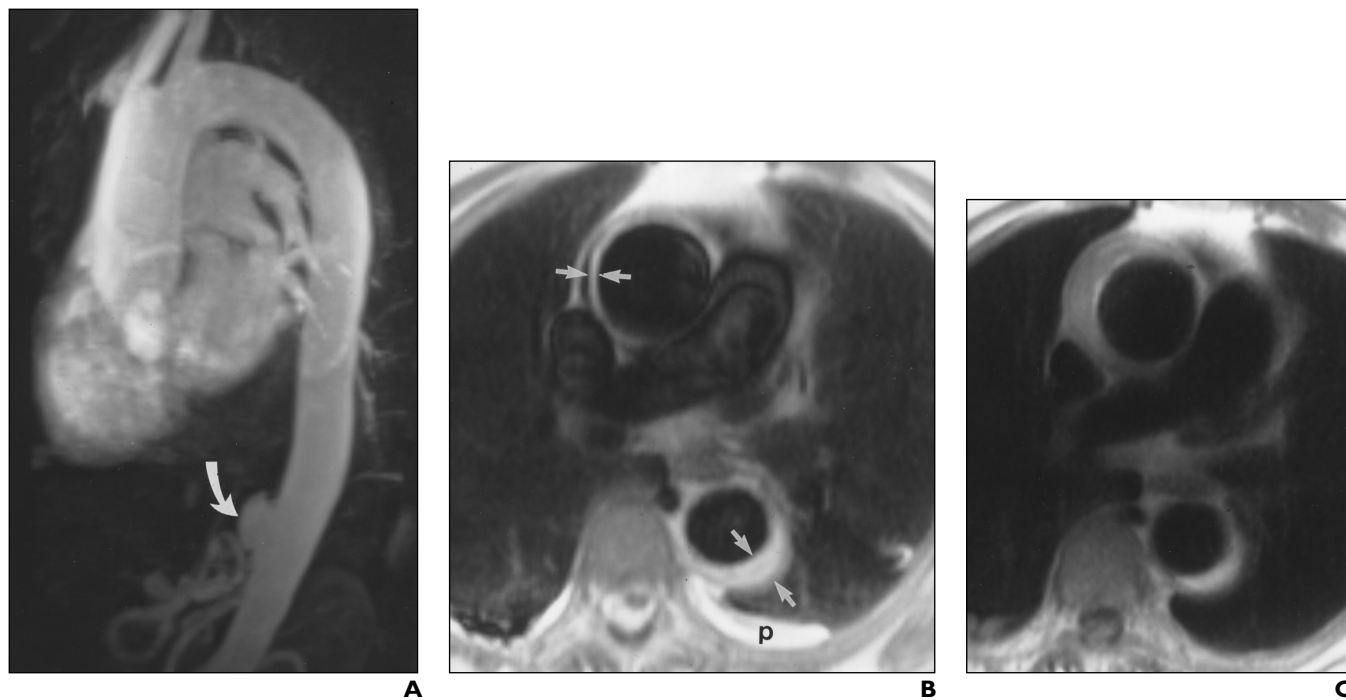

A

B

C

Fig. 7.—Intramural hematoma involving ascending and descending aorta in 72-year-old woman with hypertension and acute onset of chest and back pain.
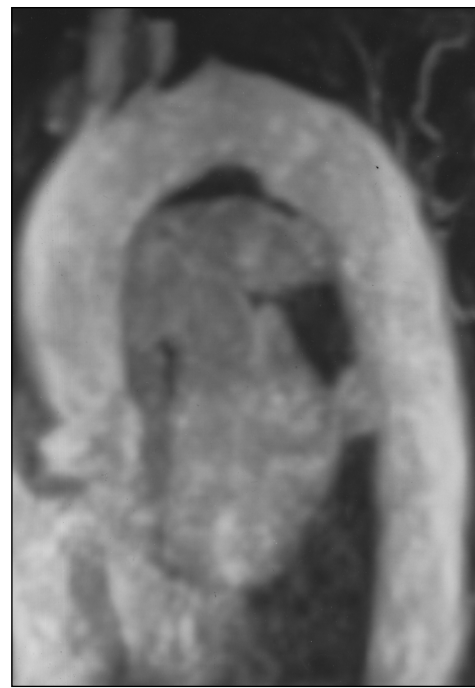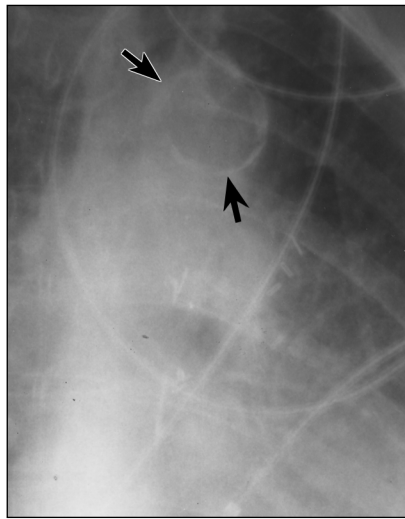
A, Oblique sagittal maximum intensity projection of gadolinium-enhanced MR angiogram of thoracic aorta shows focal penetrating ulcer in abdominal aorta (*arrow*). However, caliber and contour of thoracic aorta appear otherwise normal.

B, Axial T2-weighted half-Fourier single-shot fast spin-echo image (TR/effective TE, infinite/43) with blood-nulling inversion pulse shows thin circumferential increased signal intensity around both ascending and descending aorta (*arrows*) indicative of intramural hematoma. Small left-sided pleural effusion (p) is also shown. Likely source of intramural hematoma was penetrating ulcer. Involvement of ascending aorta usually requires surgical intervention; however, this patient was observed in hospital because of comorbidities.

C, Follow-up axial half-Fourier single-shot fast spin-echo image 1 week after **B** shows interval increase in size of ascending aorta intramural hematoma. After aggressive antihypertensive medication, patient was discharged from hospital.

Fig. 8.—Diffuse thoracic aorta calcification in 71-year-old woman who underwent subsequent coronary artery bypass grafting, which was notable for difficulty isolating noncalcified areas of aorta for implantation of bypass grafts.
A, Frontal chest radiograph shows calcified atherosclerotic plaque, best seen in aortic arch (*arrows*).
B, Oblique sagittal maximum intensity projection of gadolinium-enhanced MR angiogram of thoracic aorta shows smooth contour of aortic wall. Intimal calcification could not be detected on MR angiogram or on routine T1- and T2-weighted images.
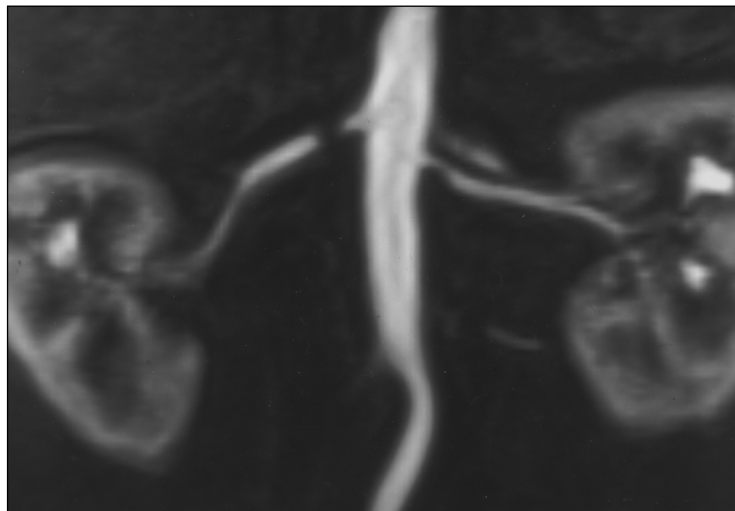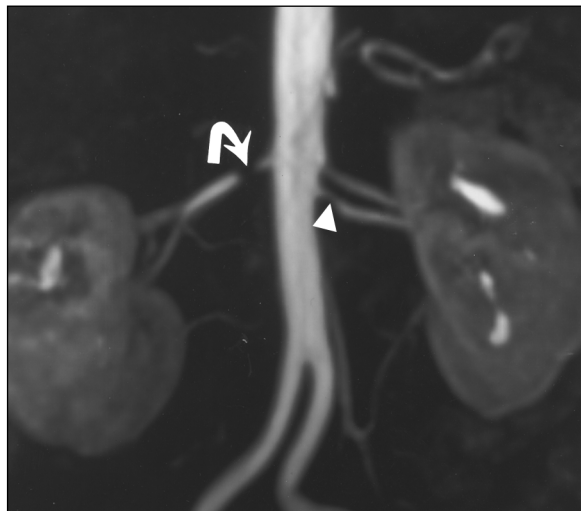
Fig. 9.—Overestimation of renal artery stenosis on MR angiography in 48-year-old woman with hypertension and suspected renovascular disease.
A, Coronal maximum intensity projection of gadolinium-enhanced MR angiogram shows occlusion of proximal right renal artery (*arrow*). Note two left renal arteries. Inferior left renal artery appears mildly to moderately narrowed proximally (*arrowhead*). Superior artery was normal on source images (not shown).
B, Oblique coronal reformatted image from MR angiogram also shows focal high-grade right renal artery stenosis. Left renal artery narrowing appears slightly less severe on source images. Note patent right iliac artery was excluded from reformatted image.
C, Angiogram shows focal high-grade stenosis of right renal artery (*arrow*). Left renal arteries are both mildly tortuous but without stenosis. In both vessels, narrowing is overestimated on MR angiography, particularly on maximum intensity projections.
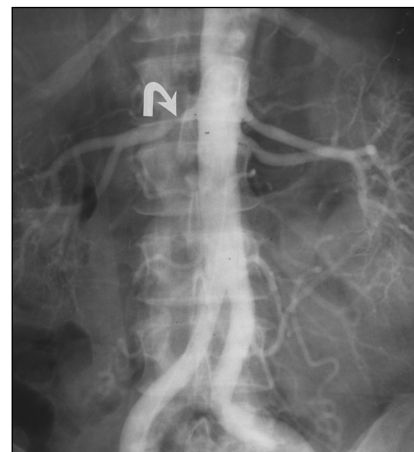
A   **B**   **C**

Fig. 10.—Metallic stent artifact in 68-year-old man who had undergone previous right common iliac artery stenting and developed new left lower extremity claudication.
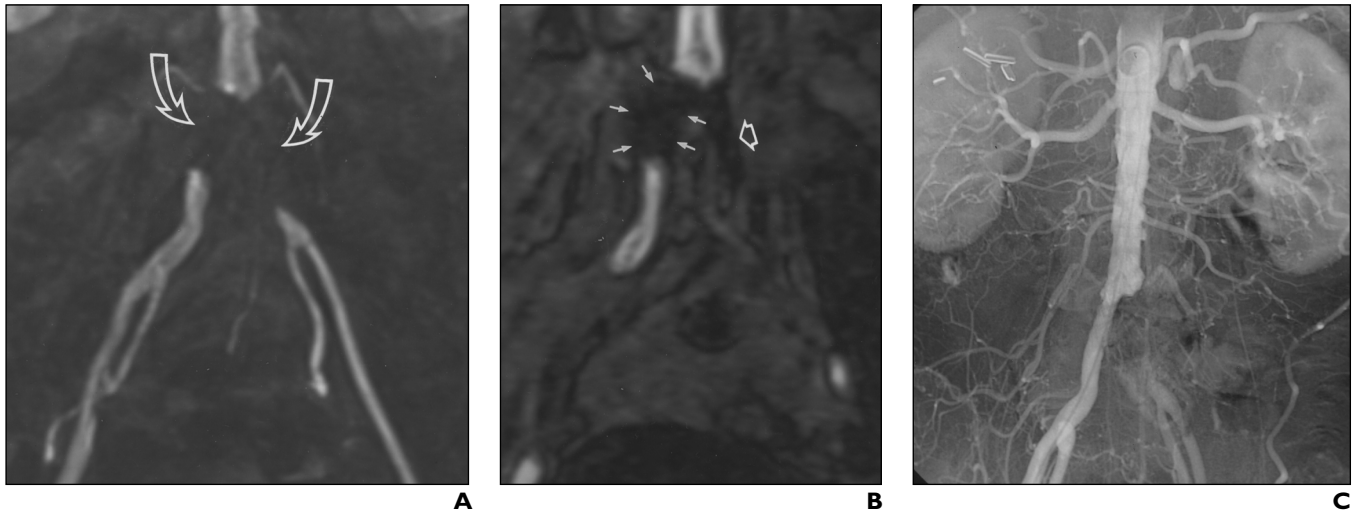**A**, Coronal maximum intensity projection of gadolinium-enhanced MR angiogram suggests bilateral common iliac occlusion (*arrows*). Note presence of "Maki" artifact (Figs. 4 and 5) in aorta and right common iliac artery. (Reprinted with permission from [9])
B, On coronal source image from MR angiogram, susceptibility artifact is seen around area of low signal intensity in right common iliac artery (*solid arrows*) unlike left (*open arrow*) and suggests that signal loss on right may be caused by metallic stent artifact.
C, Angiogram shows presence and patency of right common iliac stent. Occluded left common iliac artery has likely caused patient's new symptoms. In presence of metallic stent, patency of underlying vessel cannot be assessed definitively using MR angiography because of signal loss. (Reprinted with permission from [9])

A

Fig. 11.—Right subclavian pseudostenosis in 64-year-old man referred for evaluation of left axillary–femoral bypass graft.
A, Coronal maximum intensity projection of gadolinium-enhanced MR angiogram, obtained after IV injection of contrast material into right arm, shows contrast material in right axillary and subclavian veins (*open arrows*) and subclavian artery (*solid straight arrows*) with focal signal loss (*wavy arrow*) where vein passes adjacent to artery. T2* effects of concentrated gadolinium contrast material in vein cause susceptibility artifact affecting adjacent structures such as subclavian artery. This examination shows patency of proximal portion of left axillary–femoral bypass graft (*arrowheads*) in patient with infrarenal aortic occlusion. (Reprinted with permission from [10])
B, Coronal oblique reconstructed image of delayed three-dimensional acquisition obtained 40 sec after **A** confirms normal right subclavian artery (*arrow*). Injection into right arm was performed to avoid possible susceptibility artifacts interfering with evaluation of left axillary–femoral bypass graft anastomosis.


B

Fig. 12.—Pseudoocclusion of left popliteal artery resulting from exclusion from imaging slab in 78-year-old woman with nonhealing left foot ulcer.
A, Coronal maximum intensity projection of MR angiogram shows loss of signal in 4-cm segment of left popliteal artery (*solid arrow*) suggesting occlusion. Note mild enhancement of left saphenous vein (*open arrow*).
B, Sagittal maximum intensity projection of MR angiogram of entire imaging volume reveals that left popliteal fossa dorsal to imaging volume was inadvertently excluded from imaging slab (*arrow*). Subsequently, two-dimensional axial time-of-flight images were acquired through popliteal arteries and confirmed vessel patency (not shown). A = anterior, P = posterior.
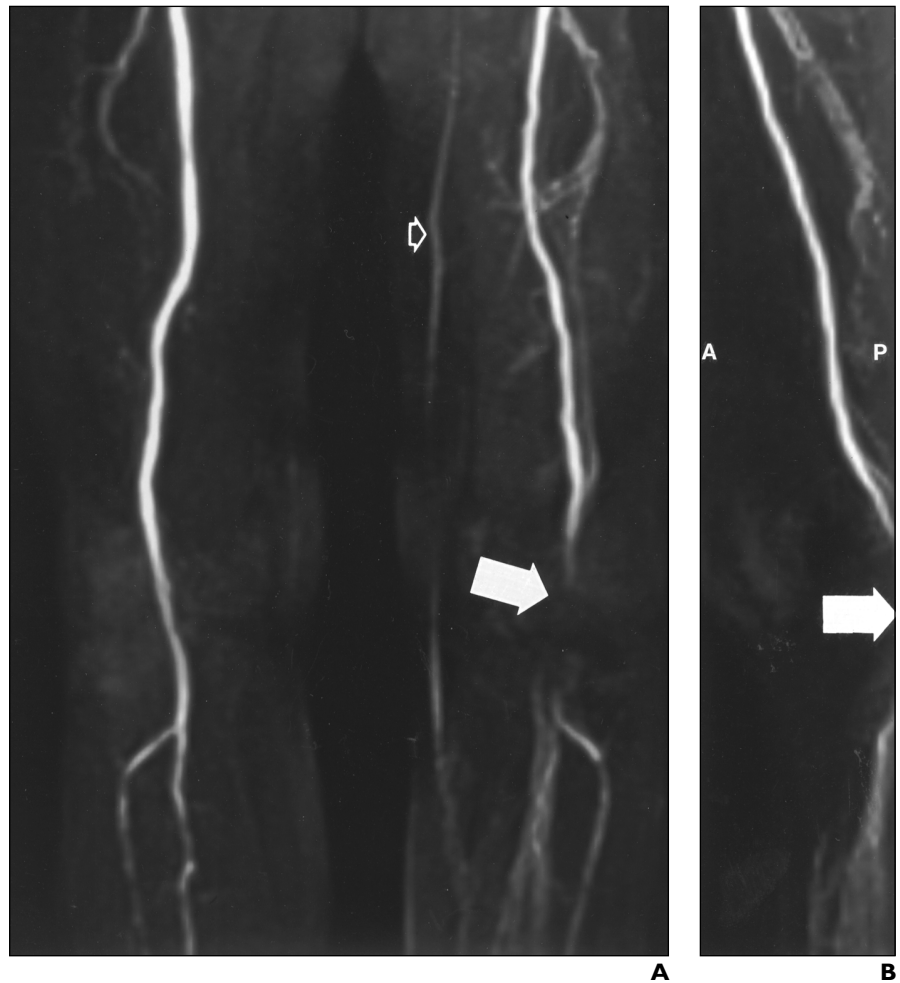
test-bolus timing examination [2]. Unenhanced images were subtracted from enhanced images, and the subtraction data set reconstructed to produce maximum-intensity-projection renderings. Both maximum intensity projections and source images with multiplanar reformatting were reviewed for interpretation.

Artifacts and Pitfalls

Mistiming of MR Acquisition

The combination of short acquisition times of about 20–25 sec and short contrast-infusion times of about 10 sec (typically 20 ml of contrast material infused at 2 ml/sec) requires precise timing to achieve high-quality angiograms without substantial venous enhancement (Fig. 1). Several methods to ensure reliable and accurate timing have been proposed, including semiautomated techniques to initiate imaging after bolus arrival [3], rapid temporally resolved acquisitions [4], and the test-bolus method [2]. The latter has the advantages of

being easy to implement and of not requiring special hardware or software.

Acquisition time too late.—Imperfectly timed acquisitions can result in variable degrees of venous enhancement in the MR arteriogram (Fig. 2). Although venous signal intensity should not affect visualization of arteries on source images, it can degrade the appearance of rendered MR angiograms such as maximum-intensity-projection images. Interestingly, this pitfall can be useful clinically if information about venous patency is desired. Large-field-of-view MR venograms can be obtained simply by subtracting arterial phase acquisitions from delayed images [5]. Although venous enhancement in MR angiography typically results from mistiming, it can also be a sign of abnormal arteriovenous shunting, such as that caused by an arteriovenous fistula (Fig. 3).

Acquisition time too early.—The acquisition of MR data (central lines of K-space in particular) before contrast bolus arrival

can produce a characteristic artifact described by Maki et al. [6] (Figs. 4 and 5). To ensure that diagnostic information is obtained despite this artifact, two three-dimensional acquisitions in rapid succession should be performed after administration of contrast medium.

Nonvisualization of Mural or Extraluminal Abnormality

The reliance on gadolinium-enhanced angiography as the sole MR imaging sequence for diagnosing vascular abnormalities can be dangerous. As on conventional angiography, the caliber of aneurysms can be substantially underestimated if mural thrombosis results in a normal lumen diameter (Fig. 6). Similarly, vasculitis and dissections or intramural hematomas can be missed on gadolinium-enhanced MR angiography (Fig. 7). Imaging protocols of the aorta must, therefore, include unenhanced spin echo (or fast spin echo) of the thoracic aorta (Fig. 7) or contrast-enhanced T1-weighted imaging of the abdomen and pelvis (Fig. 6).

A special case of nonvisualization deserves mention: invisible by MR imaging, extensive calcified atheromatous disease can complicate surgical and interventional approaches and place patients at increased risk for vascular injury and embolic complications (Fig. 8).

Overestimation of Stenosis

As with all MR angiographic methods, although to a lesser degree, gadolinium-enhanced MR angiography overestimates vessel narrowing because of spin dephasing caused by turbulent flow at a stenosis and partial volume

effects. This problem can be further exaggerated by maximum-intensity-projection reconstructions in which subtle vascular signal at stenoses cannot be distinguished from background signal [7] (Fig. 9). Image analysis should rely on an assessment of source images.
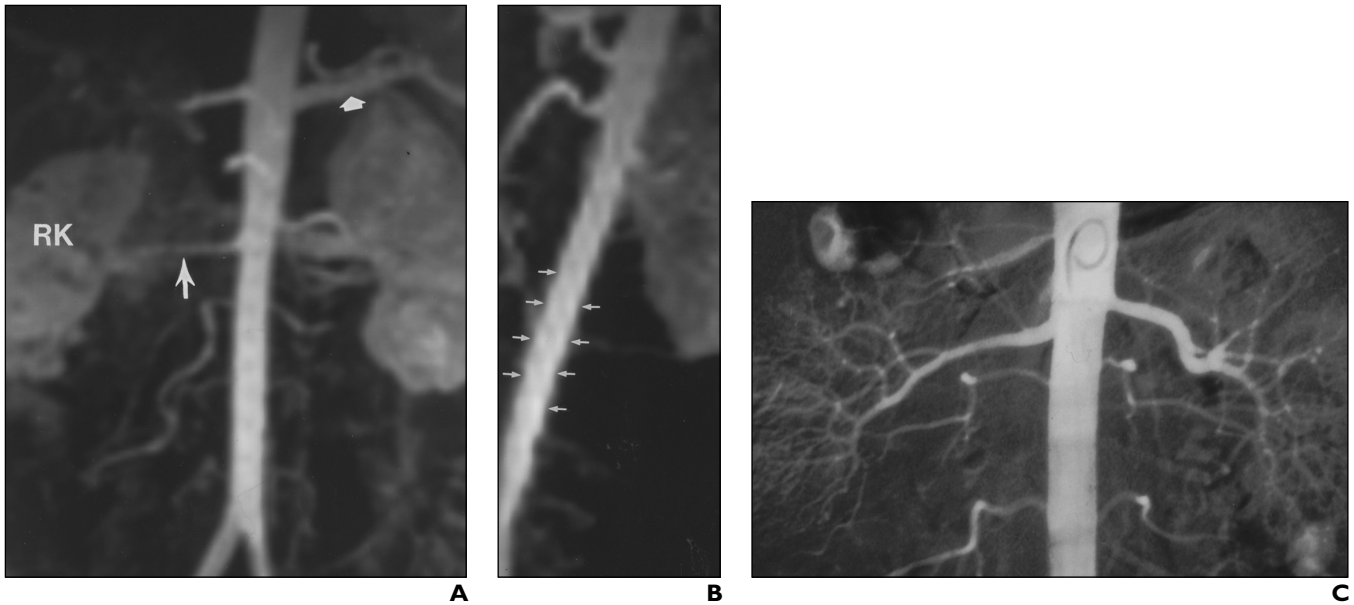

Fig. 13.—Pseudofibromuscular dysplasia in 43-year-old woman with hypertension and suspected renovascular disease.
A, Coronal maximum intensity projection of gadolinium-enhanced MR angiogram shows asymmetry in kidney sizes and lobulated contour of right kidney (RK). Right renal artery (*longer arrow*) and splenic artery (*short arrow*) have beaded appearance suggesting fibromuscular dysplasia. Slice thickness for image acquisition was 3.5 mm
B, Sagittal maximum intensity projection of MR angiogram reveals effect of using overly thick slices. "Stairstep" contour of oblique vessels, best seen in aorta (*arrows*), causes beaded appearance of vessels on coronal view.
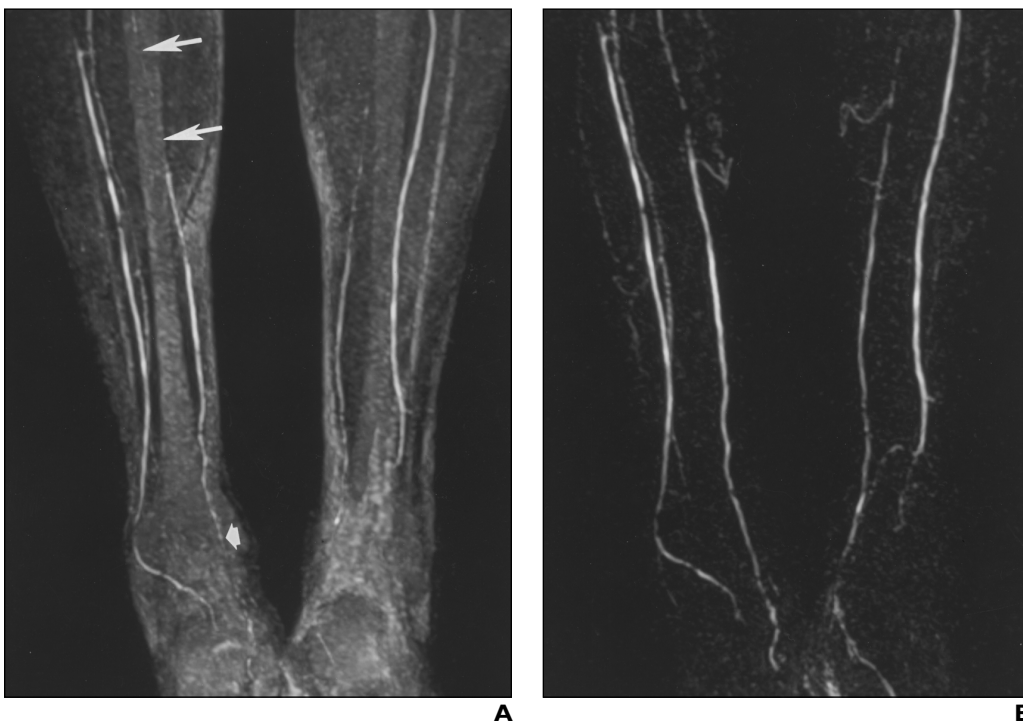**C,** Angiogram reveals normal renal arteries bilaterally.

Fig. 14.—Peripheral vessels in 76-year-old man obscured by high signal intensity from bone marrow and subcutaneous fat.
A, Coronal maximum intensity projection of unsubtracted gadolinium-enhanced MR angiogram of calves suggests long-segment occlusion of posterior tibial artery proximally (*long arrows*) and termination of posterior tibial artery above ankle (*short arrow*).
B, Coronal maximum intensity projection of gadolinium-enhanced MR angiogram after subtraction of unenhanced acquisition from **A** shows improved visualization of vessels. Although diseased, right posterior tibial artery is patent to pedal arch.

Pseudostenosis and Other Pseudolesions

Metallic artifacts.—Susceptibility artifacts arising from metallic stents, joint prostheses, and surgical clips can cause signal loss within a vessel that mimics stenosis or occlusion. Clinical history can be vital, although in certain cases, close inspection of source images may reveal a blooming or susceptibility artifact around the suspicious vessel (Fig. 10).

Subclavian or common carotid pseudolesions.—A similar susceptibility artifact can result from residual concentrated gadolinium contrast material in central veins ipsilateral to the side of injection. The T2* effect can cause adjacent signal loss and may create the false impression of arterial stenosis when veins and arteries are in close proximity (Fig. 11). Because of passage through the left subclavian and brachiocephalic veins, a left-sided injection can cause apparent stenosis of not only the left subclavian artery but also the proximal great vessels [8]. Hence, we favor injection into a right arm vein for routine thoracic MR aortography, unless right subclavian arterial abnormality is suspected. To confirm that stenoses are artifactual, delayed imaging of the artery in question should be performed (Fig. 11).

Exclusion from the imaging slab.—Vessels excluded from the imaging slab can appear falsely occluded (Fig. 12). During moving table bolus-chase examinations of the peripheral vasculature, the patient's knees should be elevated to ensure that the popliteal arteries are in the same coronal plane as the femoral arteries.

Pseudofibromuscular dysplasia.—Low image resolution with large pixel size relative to vessel size can result in inaccurate assessment of vessel caliber. In particular, it can produce a "stairstep" artifact that can mimic the beaded appearance of fibromuscular dysplasia (Fig. 13). Thin imaging of slices less than 2 mm or less should be used for renal MR angiography.

T1 Shine-Through Artifacts

Tissues other than gadolinium-enhanced vessels, such as bone marrow, fat, and hemorrhage, that have short T1 relaxation times will also have high signal intensity on MR angiography and can interfere with image interpretation. Fat-suppression techniques or image subtraction or both can be used to improve vessel visualization (Fig. 14).

References

1. Prince MR, Grist TM, Debatin JF. *3D contrast MR angiography*, 2nd ed. Berlin: Springer, **1999**
2. Earls JP, Rofsky NM, DeCorato DR, Krinsky GA, Weinreb JC. Breath-hold single-dose gadolinium-enhanced three-dimensional MR aortography: usefulness of a timing examination and MR power injector. *Radiology* **1996**;201:705–710
3. Prince MR, Chenevert TL, Foo TKF, Londy FJ, Ward JS, Maki JH. Contrast-enhanced abdominal MR angiography: optimization of imaging delay time by automating the detection of contrast material arrival in the aorta. *Radiology* **1997**;203:109–114
4. Korosec FR, Frayne R, Grist TM, Mistretta CA. Time-resolved contrast-enhanced 3D MR angiography. *Magn Reson Med* **1996**;36:345–351
5. Lebowitz JA, Rofsky NM, Krinsky GA, Weinreb JC. Gadolinium-enhanced body MR venography with subtraction technique. *AJR* **1997**;169:755–758
6. Maki JH, Prince MR, Londy FJ, Chenevert TL. The effects of time varying intravascular signal intensity and K-space acquisition order on three-dimensional MR angiography image quality. *J Magn Reson Imaging* **1996**;6:642–651
7. Anderson CM, Saloner D, Tsuruda JS, Shapeero LG, Lee RE. Artifacts in maximum-intensity-projection display of MR angiograms. *AJR* **1990**;154:623–629
8. Lee Y-J, Chung T-S, Joo J-Y, Chien D, Laub G. Suboptimal contrast-enhanced carotid MR angiography from the left brachiocephalic venous stasis. *J Magn Reson Imaging* **1999**;10:503–509
9. Rofsky NM, Johnson G, Adelman MA, Rosen RJ, Krinsky GA, Weinreb JC. Peripheral vascular disease evaluated with reduced-dose gadolinium-enhanced MR angiography. *Radiology* **1997**;205:163–169
10. Krinsky GA, Reuss PM. MR angiography of the thoracic aorta. *Magn Reson Imaging Clin N Am* **1998**;6:293–320